Subpicosecond Interfacial Charge Separation in Dye-Sensitized Nanocrystalline Titanium Dioxide Films

Yasuhiro Tachibana,[†] Jacques E. Moser,[‡] Michael Grätzel,[‡] David R. Klug,[†] and James R. Durrant*[,†]

Centre for Photomolecular Sciences, Departments of Chemistry and Biochemistry, Imperial College, London SW7 2AY, U.K., and Institut de Chimie Physique, École Polytechnique Fédérale de Lausanne, CH-1015 Lausanne, Switzerland

Received: July 23, 1996; In Final Form: October 10, 1996[⊗]

We have employed subpicosecond transient absorption spectroscopy to study the rate of electron injection following optical excitation of the ruthenium dye Ru^{II}(2,2′-bipyridyl-4,4′-dicarboxylate)$_2$(NCS)$_2$ (**1**) adsorbed onto the surface of nanocrystalline titanium dioxide (TiO_2) films. This sensitizer dye is of particular interest as it is the most efficient sensitizer dye reported to date and is receiving considerable attention for applications in photoelectrochemical solar energy conversion. Transient data collected for **1** adsorbed onto TiO_2 films were compared with those obtained for control dye-coated ZrO_2 films, as the high conduction band edge of ZrO_2 prevents electron injection. Adsorption of the dye onto the TiO_2 film was found to result in a rapid (<500 ps) quenching of the dye excited-state luminescence. Absorption difference spectra collected for the two dye-coated films were assigned by comparison with the spectroscopy of the dye excited and cation states in solution. These transient absorption data indicated that electron injection in these films occurs in $\leq 10^{-12}$ s. Detailed analysis indicates the injection is at least biphasic, with ∼50% occurring in <150 fs (instrument response limited) and 50% in 1.2 ± 0.2 ps. These ultrafast electron injection kinetics are contrasted with the charge recombination reaction, which occurs on the microsecond−millisecond time scales. The ultrafast rate of electron injection observed here is critical both for the high energy conversion efficiencies obtained with this sensitizer dye, and for the excellent long-term stability of this dye in photoelectrochemical solar cells.

Introduction

Wide-bandgap semiconductors may be sensitized to visible light by the adsorption of dyes to their surface. This process is employed commercially in, for example, most modern electrophotographic and photographic processes.[1,2] It is also now used in a new generation in photovoltaic devices based upon dye-sensitized nanocrystalline titanium dioxide (TiO_2) thin films. These photoelectrochemical solar cells have already achieved >10% energy conversion efficiencies[3,4] and are attracting considerable commercial interest due to their potential for low production costs. However, despite the considerable technological importance of dye sensitization, detailed studies of the kinetics and mechanism of this process have to date been very limited.[5]

The photovoltaic function of these solar cells is based upon the light-induced separation of charge at the dye/semiconductor interface, as illustrated in Figure 1. Optical excitation of the dye molecule results in electron injection into the semiconductor conduction band. Efficient sensitization requires that the rate of this interfacial electron transfer be much greater than the rate of decay of the dye excited state to ground. The kinetics of these processes are therefore a critical factor controlling device efficiency.[5] However, interfacial electron-transfer reactions remain poorly characterized relative to homogeneous solution or gas-phase electron transfer.[6] The electron transfer involves the coupling of the localized molecular excited state of the dye to highly delocalized electronic levels of the semiconductor conduction band, providing a significant conceptual challenge

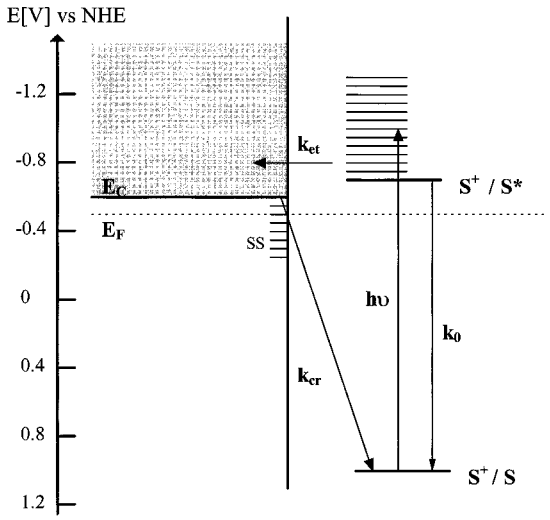

Figure 1. Schematic representation of charge separation in the dye-sensitized TiO_2 thin films. Optical excitation of the Ru^{II}(dcbpy)$_2$(NCS)$_2$ (**1**) dye (S° → S*) at 600 nm initiates ultrafast electron injection (k_{et}) into the TiO_2. Electron-acceptor states of the semiconductor include both surface states (SS) and delocalized conduction band states. Charge recombination (k_{cr}) between the resulting TiO_2 electron (e_{cb}^-) and oxidized dye molecule (S^+) occurs relatively slowly. In the functioning photovoltaic cell, the addition of appropriate electrodes and electrolyte complete the electrical circuit and result in forward electron transport with a near-unity quantum yield. k_0 indicates radiative and radiationless decay of S* to S°. The potential level scale is with respect to NHE. In this study we demonstrate that k_{et} is $10^{12}-10^{13}$ s^{-1}, $k_0 \sim 10^8$ s^{-1}, and k_{cr} 10^6-10^3 s^{-1}, thus ensuring efficient charge separation in photovoltaic cells in employing this sensitizer dye.

* Corresponding author: Centre for Photomolecular Sciences, Department of Biochemistry, Imperial College, London, SW7 2AY, Fax (44) 171 594 5806, e-mail J.Durrant@ic.ac.uk.
† Imperial College.
‡ École Polytechnique Fédérale de Lausanne.
⊗ Abstract published in *Advance ACS Abstracts,* December 1, 1996.

S0022-3654(96)02227-7 CCC: $12.00

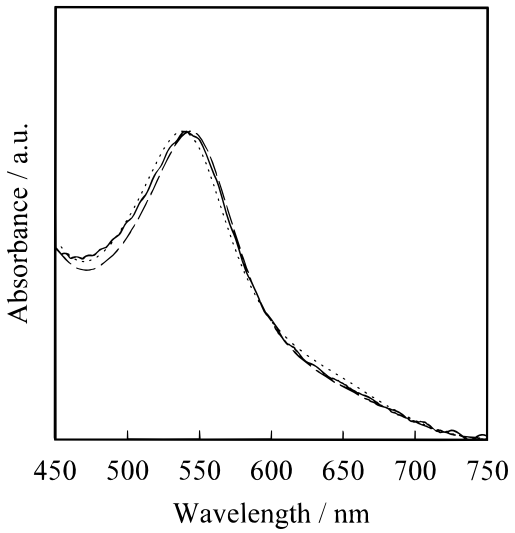

Figure 2. Absorption spectra of **1** in ethanol (···) and the same dye adsorbed onto the surface of a nanocrystalline TiO_2 (—) and ZrO_2 (– – –) films. Spectra were normalized to the absorbance maximum at 538 nm, after subtraction of the spectra obtained for undyed films, and were uncorrected for scatter.

in describing the mechanism of this reaction. Theoretical studies[6−8] have suggested that if good energetic overlap is achieved between the dye excited state and the conduction band, then the electron injection reaction may be activationless and proceed with rates of $10^{12}-10^{14}$ s^{-1}. However experimental studies on these time scales have been very limited.[6]

Of all potential sensitising dyes for photoelectrochemical solar cells, ruthenium(II) trisbipyridyl ($Ru(bpy)_3^{2+}$) complexes and their analogues have received the most attention.[5,9] The optimum energy conversion reported to date for a photoelectrochemical solar cell has been obtained using the sensitizer dye Ru^{II}(2,2′-bipyridyl-4,4′-dicarboxylate)$_2$(NCS)$_2$, (Ru^{II}(dcbpy)$_2$-(NCS)$_2$, **1**).[4] The carboxylate groups result in strong binding of this dye to the TiO_2 surface, while the NCS groups enhance the visible absorption of the dye. Optical excitation of **1** adsorbed onto the surface of TiO_2 results in electron injection with a near unity quantum yield.[4] In functioning photoelectrochemical solar cells, the resulting dye cation is reduced by an electrolyte containing a I^-/I^{3-} redox couple, while the injected electron is transported through the nanocrystalline film to a back electrode. The dye exhibits excellent stability, sustaining more than 10^8 turnovers without significant degradation of the energy output of the cell. This high stability has been attributed, at least in part, to ultrafast electron injection competing very effectively with degradation pathways from the dye excited state.[4]

The ground-state absorption spectrum of **1** in solution is shown in Figure 2. This spectrum is dominated by an absorption band at 538 nm, with a long wavelength tail extending out to 750 nm. Luminescence from this dye exhibits a maximum at 755 nm, with a luminescence decay time of 50 ns in degassed ethanol solution.[4] These spectral characteristics are typical of analogous $Ru(bpy)_3^{2+}$ complexes, although red-shifted by the inclusion of the NCS^- ligands in the complex. Picosecond resonance Raman studies have indicated that optical excitation of $Ru(bpy)_3^{2+}$ result in formation of the state $[Ru^{III}(bpy)_2bpy^-]^{2+}$, with localization of the excited electron on a bipyridyl ligand and vibrational relaxation being complete within ∼6 ps.[10−12] On the basis of analogies with these and other studies,[9] the 538 nm absorption band observed for **1** has been assigned to a $t_{2g} \rightarrow \pi^*$ metal-to-ligand charge-transfer (MLCT) transition.[4] The $[Ru^{III}(bpy)_2bpy^-]^{2+}$ excited state is weakly luminescent, decaying on the nanosecond time scale.[9] Low-temperature studies have indicated that on this time scale this state comprises a manifold of MLCT (d, π^*) states of primarily triplet character.[9,12] The weak long-wavelength absorption tail which is typical of these complexes has been attributed to direct excitation of this luminescent state.[9]

There have been no studies reported of the kinetics of electron injection employing **1** as a sensitizing dye, although there have been several studies of nanocrystalline TiO_2 sensitized by related dyes. These have, however, reported widely differing time constants for electron injection: <7 ps for $Ru(dcbpy)_2(H_2O)_2^{2+}$,[13] 172 ps for trinuclear $Ru(dcbpy)_2(CN)_2$,[14] and 5 ns for $Ru(dcbpy)(bpy)_2^{2+}$.[15] Sakata and co-workers have reported with time constants ranging from 10^{-9} to 10^{-6} s for $Ru(bpy)_3^{2+}$ adsorbed onto TiO_2 powders.[16] At present there is no consensus over the time scale of electron injection from this class of dye, nor indeed whether all dyes of this class with similar excited-state redox energies should be expected to exhibit similar electron injection kinetics.

In this paper, we present a detailed study with subpicosecond time resolution of the kinetics of electron injection in nanocrystalline TiO_2 films sensitized by **1**. By employing the dye-sensitized films used in commercial photoelectrochemical solar cells, we ensure that our measurements are directly related to the function of these devices. These studies are complemented by ultrafast spectroscopic study of **1** in solution and adsorbed on a nonquenching substrate. For the latter purpose we chose nanocrystalline zirconium dioxide (ZrO_2) films. ZrO_2 has a similar surface and optical properties to TiO_2, but a conduction band potential ∼1 V more negative than TiO_2, thus inhibiting electron injection.[17] The time resolution of these experiments (150 fs) has allowed the study of interfacial electron transfer on subpicosecond time scales in a system of technological importance. A brief summary of some of these results has been reported previously.[18]

Materials and Methods

Nanocrystalline TiO_2 and ZrO_2 films (thickness 8 μm) sensitized by **1** were prepared as previously (Method A of ref 4). Adsorption of the dye was achieved by immersion of the film in room-temperature ethanol solution of **1** (2×10^{-5} M) for 4 h, resulting in a dye optical density at 538 nm of ∼0.2. The films were covered with ethylene carbonate/propylene carbonate (1:1) solution and thin cover glasses by capillary forces. The samples were stored in the dark under anhydrous conditions; all experiments were conducted at room temperature.

The nanosecond−millisecond transient absorption and luminescence experiments employed a nitrogen laser pumped dye laser to generate 510 nm excitation pulses (0.3 mJ/cm^2) at 2 Hz. These excitation conditions resulted in excitation of approximately 3% of the dye molecules per pulse. For the absorption measurements, the probe light source was a tungsten lamp or pulsed xenon arc lamp (15 μs pulse length). Appropriate monochromators and/or filters were used to minimize the probe light incident upon the sample. For the emission data, all luminescence at wavelengths >660 nm was collected, selected by a Schott glass high-pass filter. Transient data were collected with a photodiode and digitized using a Gould 475 digital oscilloscope. The instrument response of the apparatus was 4 ns fwhm. Subpicosecond transient absorption spectroscopy was carried out as previously.[19] Samples were excited at 605 nm (∼0.4 mJ/cm^2, spot diamter 200 μm) with the magic angle configuration (ca. 54.7°) between pump and probe pulses at a repetition rate of 6.5 kHz. Some data were collected with the sample spun at 60 Hz, such that the sample volume was

replaced between excitation pulses. Data collected with and without spinning were indistinguishable, indicating negligible accumulation of long-lived species between excitation pulses. Transient absorption spectra were collected as a function of time delay using a multichannel detector. A dye standard (Nile Blue in methanol) was used to determine the instrument response (150−250 fs rise time depending upon probe wavelength) and zero time delay of the spectrometer. Transient absorption data were collected over two time scales of 0−3 and 0−12 ps with a time delay of 16.7 and 66 fs between points, respectively. Data were globally analyzed as previously[19] assuming multiexponential kinetics after deconvolution with the instrument response.

All transient data collected with the dye-coated TiO_2 and ZrO_2 films have been scaled to take account of different dye optical densities of these films at the excitation wavelength used in each experiment, allowing quantitative comparison of amplitudes of the transient data collected with these two sample types. Moreover, for all experiments, control data were collected with undyed nanocrystalline films in order to determine the magnitude of signals arising from excitation of intraband states of the semiconductor. In all cases the undyed films exhibited negligible transient signals (<10% of the signals observed for the dye-coated films).

The integrity of every sample was assayed before and after all optical experiments by steady-state absorption and/or transient absorption spectroscopy. The dye excited state can be readily distinguished from the state $dye^+e_{CB}^-$ by nanosecond transient absorption spectroscopy (see Results), and this therefore comprises an assay of the electron injection efficiency of each sample. Light induced degradation of the dye-sensitized TiO_2 films resulted in the appearance of a ∼10 ns component in the transient data attributable to excited-state decay of dyes unable to inject electrons into the TiO_2. Prolonged storage of the films, particularly in the absence of the PC/EC solution, resulted in a shift in the dye absorption maximum to ∼500 nm. This blue-shift is most probably associated with an oxygen-dependent desulfurization reaction of the NCS ligands.[20] For all results presented here, the samples exhibited absorption maxima at 538 ± 2 nm before and after all experiments and, in the case of the TiO_2 films, were shown to exhibit injection yields near unity.

Results

Figure 2 compares the absorption spectra of $Ru^{II}(dcbpy)_2(NCS)_2$ (**1**) in ethanol with that of the dye adsorbed onto the nanocrystalline TiO_2 and ZrO_2 films. Absorption to the films results in only slight change in the dye absorption spectrum, in contrast to results which have been reported for other sensitizer dyes (e.g., $Ru(dcbpy)(bpy)_2^{2+}$ [21]).

Luminescence Data. Figure 3 compares the nanosecond luminescence decay kinetics of **1** adsorbed onto TiO_2 and ZrO_2 films. The ZrO_2 films exhibits biexponential decay kinetics on the nanosecond time scale (lifetimes of 3 and 25 ns), similar to those observed for the dye in solution, and attributed to decay of the dye excited state to ground (the slower time 50 ns constant reported previously[4] was obtained with degassed solutions). In contrast, luminescence from the dye-coated TiO_2 film is strongly quenched, with its decay being primarily instrument response limited. From the extent of the quenching observed for the dye-coated TiO_2 film, we conclude that the lifetime of the dye luminescent excited state in the TiO_2 films is <500 ps. This is only an upper limit for this excited-state lifetime, as luminescence from TiO_2 intraband states[14] and/or from a small subpopulation (<10%) of unquenched dye molecules may also contribute to the small residual signal.

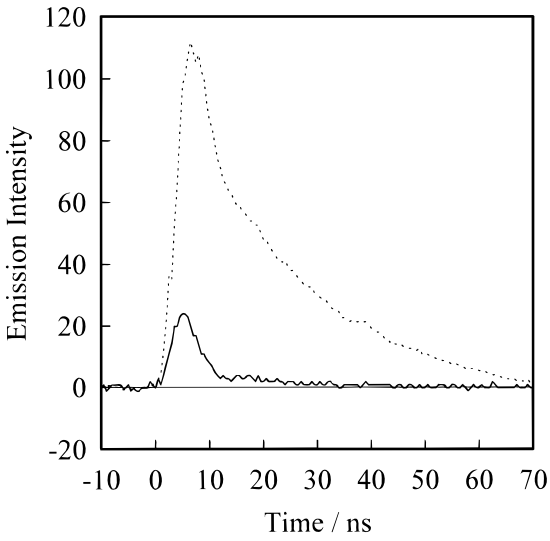

Figure 3. Nanosecond emission decay kinetics for the TiO_2 (—) and ZrO_2 (···) films coated by **1**. Luminescence from the dye coated ZrO_2 films exhibits biexponential decay kinetics with time constants of ∼3 and 25 ns. Luminescence from the dye-coated TiO_2 films is strongly quenched and dominated by a fast, instrument response limited decay. A small-amplitude nanosecond decay can also be resolved. The quenching of dye luminescence observed for the TiO_2 film indicates that the dye excited-state lifetime on these films is <500 ps.

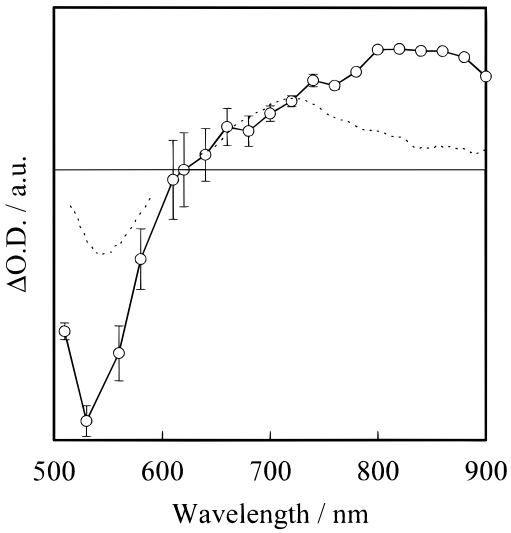

Figure 4. Absorption difference spectra of the formation of cation (○) and excited (···) states of **1** in ethanol solution. The difference spectrum for the excited state is taken at a time delay of 5 ps after 605 nm excitation in the absence of any electron acceptors. The cation state spectrum was obtained at a time delay of 10 μs after excitation of **1** in the presence of the electron acceptor methylviologen (MV). The spectrum does not contain any residual contributions from the dye excited state which decays within nanosecond time scale. Contributions to this difference spectrum of the MV anion have been subtracted from the transient data.

Absorption Difference Spectra: Solution Phase. Figure 4 shows absorption difference spectra due to the formation of excited and cation states of **1** in ethanol solution. The difference spectrum for the dye excited state, obtained at a time delay of 5 ps, exhibits both bleaching of the ground-state absorption (500−600 nm) and the appearance of excited-state absorption, with a positive maximum at 720 nm. The magnitude of this positive maximum is proportional to the number of NCS ligands included in this complex.[20] This excited-state absorption may therefore be associated with a ligand-to-metal charge-transfer transition (LMCT) from the $(NCS)^-$ ligands to the Ru^{3+} metal center of the dye excited state. The dye cation difference

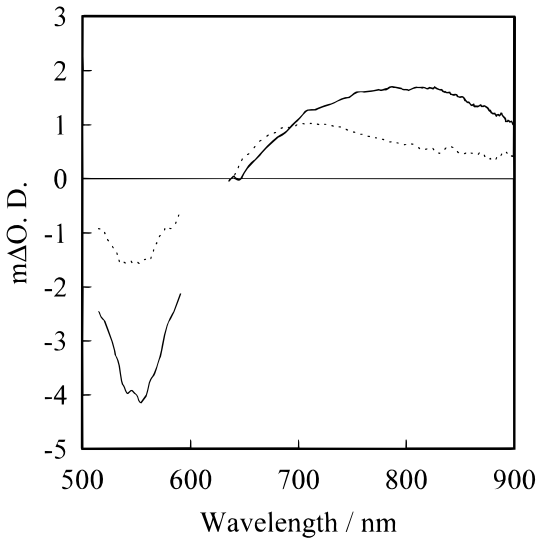

Figure 5. Absorption difference spectra obtained for TiO_2 (—) and ZrO_2 (···) coated by **1** taken at a time delay of 5 ps after 605 nm excitation. The spectrum obtained for the dye-sensitized ZrO_2 film exhibits a maximum at 710 nm as observed for **1** in ethanol solution and is therefore assigned to the dye excited state. In contrast for the dye-coated TiO_2 film this maximum is red-shifted to 800 nm as observed for the dye cation state in ethanol solution. Therefore this spectrum is assigned to the charge separated state $dye^+e_{cb}^-$ formed by electron injection from the dye excited state into the TiO_2.

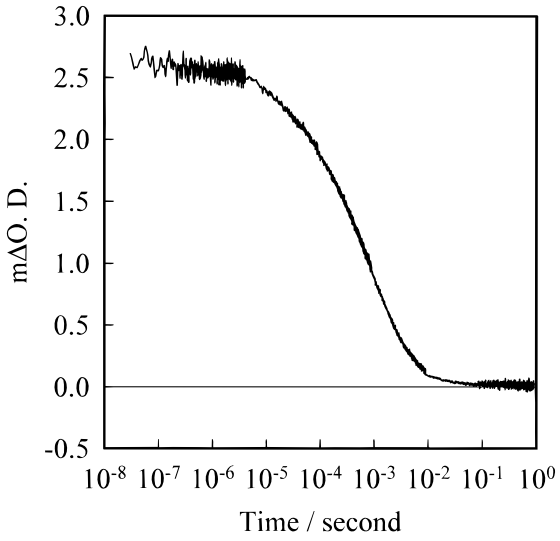

Figure 6. Kinetics of charge recombination the dye-coated TiO_2 film, monitored by decay of the cation absorption band at 820 nm. The data are shown on a lin/log plot and exhibit multiphasic kinetics on the microsecond−millisecond time scales.

spectrum was obtained by excitation of **1** in the presence of the electron acceptor methylviologen (MV) and taken at a time delay of 10 μs, to avoid any residual contributions from the dye excited state. Optical excitation of $Ru(bpy)_3^{2+}$ in the presence of MV has previously been shown[22] to generate the $Ru(bpy)_3^{3+}$ and MV^- ions with a quantum yield of up to 0.4. Contributions to the experimental data resulting from formation of the MV anion have been subtracted from the transient data,[23] yielding the cation spectrum as shown in Figure 4. This cation difference spectrum also exhibits bleaching of ground-state absorption but can be readily distinguished from the excited state by a red-shift of the positive absorption maximum to 800−850 nm.

Absorption Difference Spectra: Nanocrystalline Films. Absorption difference spectra obtained for TiO_2 and ZrO_2 films coated with **1** are shown in Figure 5. These spectra were taken at a time delay of 5 ps; however, similar spectra were also obtained from data collected on nanosecond time scales. Comparison of Figures 4 and 5 readily allows assignment of these spectra. The spectrum obtained for the dye-coated ZrO_2 film exhibits a peak at 710 nm, as observed for **1** in solution, and is therefore assigned as above to the dye MLCT excited state. In contrast the spectrum obtained with the dye coated TiO_2 film exhibits a red-shift of this peak to 800 nm, as observed for cation state of **1** in solution and is therefore assigned to the formation of this state. The formation of the dye cation state in this film is presumably coincident with the appearance of a conduction band electron in the TiO_2 (e_{cb}^-). However such electrons exhibits only relatively weak absorption throughout this spectral region[24] ($\epsilon_{780} \sim 3400\ M^{-1}\ cm^{-1}$). This e_{cb}^- absorption may contribute to the positive absorption observed in the near-infrared but cannot be separated from absorption by the dye cation in these experiments.

The transient absorption spectra taken for the dye-coated films were taken under identical excitation conditions and have been normalized to take account of small differences in optical density at the excitation wavelength. These spectra therefore correspond to those obtained for equal excited-state populations and may be quantitatively compared, as discussed below. The smaller signal observed between 500 and 600 nm for the dye-coated ZrO_2 film is attributed to overlap of the negative ground-state bleach with positive signals associated with the LMCT and bipyridyl anion $\pi \rightarrow \pi^*$ absorption of the dye excited state.

Transient Absorption Kinetics. The transient absorption spectra obtained with the dye-sensitized ZrO_2 films decayed on the nanosecond time scale, with kinetics indistinguishable from those observed in the luminescence data (data not shown). Similar transient spectra were obtained for all delays greater than the apparatus instrument response (150−250 fs) up to the nanosecond time scale.

Adsorption of **1** onto the TiO_2 film resulted in a much slower, multiphasic recovery of the cation absorption, (Figure 6), attributed to charge recombination from the $dye^+e_{cb}^-$ on the microsecond−millisecond time scales. The recombination kinetics shown in Figure 6 were found to be somewhat variable between samples, and a detailed study of these kinetics will be reported elsewhere. However, for all samples a significant proportion of this recombination occurred on time scales as slow as 1 ms, while only a small proportion of the recombination occurs on the nanosecond time scale. Similar multiphasic recombination kinetics have previously been reported[25] for $Ru(dcbpy)_3^{2+}$-sensitized nanocrystalline TiO_2 films and attributed to the disordered nature of the film (specifically electron tunneling between trap states of the semiconductor)

In contrast to the data obtained for the dye-coated ZrO_2 films, the difference spectra obtained with TiO_2 dye-coated films exhibited some temporal evolution for time delays less than 5 ps. Typical transient absorption data at a probe wavelength of 750 nm is shown in Figure 7a, while Figure 7b shows transient spectra at time delays of 150 fs, 1 ps, and 10 ps. Global analyses of transient absorption kinetics obtained at 600 probe wavelengths indicated these data could be well fit by an exponential component with a lifetime of 1.2 ± 0.2 ps in addition to a nondecaying component. Similar lifetimes for this component were obtained for all spectral regions. The spectrum of the amplitude of this component is shown in Figure 8, and its assignment is discussed below.

Discussion

The dye-coated nanocrystalline TiO_2 films used in this study were prepared using the same procedures and the same

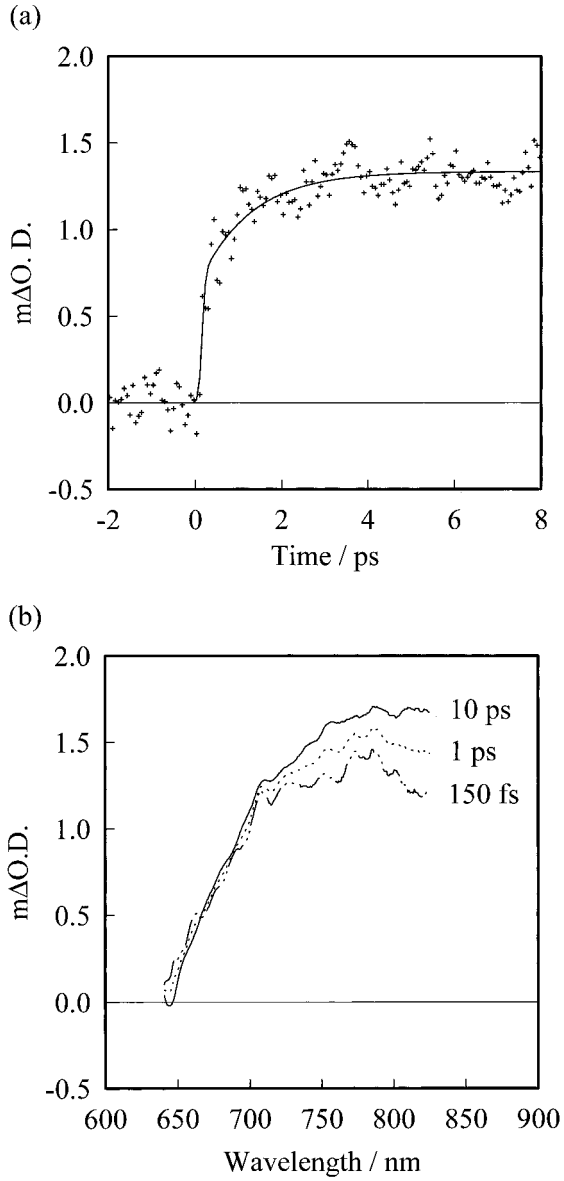

Figure 7. Subpicosecond transient absorption data obtained for the dye-coated TiO_2 films. (a) Kinetics monitored at 750 nm. The solid line is a fit to the data, after deconvolution of the instrument response, corresponding to a 1.2 ± 0.2 ps exponential grow in, and a long-lived offset signal. (b) Transient spectra obtained at time delays of 150 fs, 1 ps, and 10 ps.

sensitising dye, $Ru^{II}(dcbpy)_2(NCS)_2$ (**1**), as employed in commercial photoelectrochemical solar cells. Thus the results presented here are of direct relevance to the function of these devices. However, the choice of this experimental system has necessitated a careful study of not only the sensitized film but also the isolated dye in solution, as no transient absorption data have been reported previously for this dye. Particular care was taken to ensure the functional integrity of each sample before and after ultrafast spectroscopic study (as detailed in Materials and Methods). Moreover, the use of an nonquenching control film (dye-coated nanocrystalline ZrO_2) allows us to discriminate between changes in the transient data resulting solely from incorporation of the dye into a nanocrystalline film and changes specifically associated with electron injection.

The transient absorption and luminescence data indicate that the photophysics of **1** adsorbed onto the ZrO_2 film is very similar to that observed in solution. This is consistent with previous studies of dye coated ZrO_2 films, which have also concluded that the 1 eV shift of the conduction band edge of ZrO_2 relative

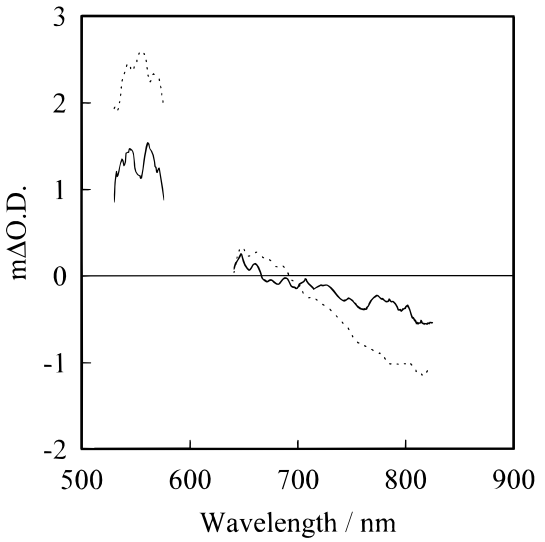

Figure 8. Spectrum of the amplitude of the 1.2 ps component observed with the dye-coated TiO_2 film (—). Also shown is the spectrum expected for the absorption changes associated with electron injection (···) obtained by taking the difference between the two spectra shown in Figure 5 assigned to the dye excited state and the charge-separated state $dye^+e_{cb}^-$. It is apparent that the spectrum of the 1.2 ps component is very similar to that expected for electron injection but has only approximately 50% of the expected amplitude.

to TiO_2 inhibits electron injection in these films. We thus conclude that optical excitation of this dye adsorbed onto ZrO_2 results in generation of the dye excited state. In contrast the data we have obtained for the dye-coated TiO_2 film indicate that in this sample electron injection occurs from the dye into the TiO_2 conduction band, with at least 90% of the dye excited states being quenched by electron injection again within a few picoseconds. This high yield for electron injection is consistent with previous photoelectrochemical studies of TiO_2 films sensitized by this dye, and with the high energy conversion efficiencies achieved with photovoltaic solar cells employing such films.[4]

Dye Photophysics. The excitation pulses used in our ultrafast experiments were at 605 nm, in the long-wavelength tail of the 538 nm absorption band of **1**. Previous studies of analogous $Ru(bpy)_3^{2+}$ dyes (see Introduction) suggest that these excitation conditions could result both in excitation of the singlet MLCT state corresponding to this 538 nm transition and in excitation of low oscillator strength transitions responsible for the long-wavelength tail. The presence of the fluorescent singlet excited state of **1** could be readily detected in our data by presence of stimulated emission from these state. No such stimulated emission is observed,[26] indicating either that our 605 nm excitation results in only a negligible population of this state or that any such state populated during our experiments has decayed within our time resolution (150 fs) to states with only weak radiative coupling to the ground state. Ultrafast relaxation of the singlet state is also consistent with the absence of fluorescence from this state in the steady-state emission spectrum of this dye, and with the results of picosecond Raman studies[10] of $Ru(bpy)_3^{2+}$.

Kinetics of Electron Injection. Our assignment of the absorption difference spectrum obtained 5 ps after excitation of TiO_2 films coated with **1** to the state $dye^+e_{cb}^-$ indicates that electron injection occurs in <5 ps. This conclusion is supported by our transient luminescence data, which indicate that decay of the dye excited state in these films occurs in less than 500 ps. Detailed analysis (see below) of our transient data at early times indicates that the electron injection is in fact at least

biphasic, as discussed below, with ~50% occurring in <150 fs and the remainder in ~1.2 ps.

Electron injection should appear in the transient absorption data as a loss of transient absorption signals resulting from the dye excited state, and the concomitant appearance of signals resulting from the state $dye^+e_{cb}^-$. We have assigned the two difference spectra shown in Figure 5 to these two states, and it follows that any kinetic component associated with electron injection should exhibit a wavelength dependence corresponding to the difference between these two spectra. Figure 8 compares this expected spectrum for the electron injection with the spectrum of the amplitude of the 1.2 ps component observed with the dye-coated TiO_2 film. It is apparent that the shape of these spectra are indistinguishable, and we therefore assign the 1.2 ps component to electron injection from the adsorbed dye into the TiO_2.

While the shape of the 1.2 ps is indistinguishable from that expected for electron injection, its amplitude is only 50 ± 5% of that expected. It can thus be concluded that this component is associated only with ~50% of the electron injection. A similar conclusion may also be reached by from the transient spectrum at 150 fs (Figure 7b), which exhibits a broad, flat positive absorption between 700 and 800 nm, consistent with an approximately 50/50 mix of the spectra assigned to the dye excited and $dye^+e_{cb}^-$ states. It can thus be concluded that the remaining 50% of the electron injection occurs in less than 150 fs.

As discussed above, no stimulated emission from fluorescent excited states of **1** could be resolved in our experiments. As the fast phase of electron injection occurs within our time resolution, we are unable to determine whether this phase of electron injection proceeds before or after relaxation of the dye excited state. However, the spectrum of the 1.2 ps component (Figure 8) is consistent with this slow phase of electron injection proceeding from the weakly luminescent excited state observed for the dye-coated ZrO_2 films on the picosecond and nanosecond time scales. It is possible that the 150 fs phase of electron injection proceeds directly from the initially excited singlet state, while the 1.2 ps phase proceeds from the relaxed excited state, although additional data are needed to establish this issue. It should also be noted that given the signal-to-noise limitations of our experiment, a more complex distribution of electron injection times cannot be ruled out.

Comparison with Other Studies. Our conclusion that electron injection occurs on a picosecond and subpicosecond time scales is consistent with conclusion of Willig and co-workers that electron injection in $Ru(dcbpy)_2(H_2O)_2^{2+}$-sensitized nanocrystalline TiO_2 films occurs in <7 ps. Similar subpicosecond excited-state quenching has also been reported for adsorption of coumarin dye onto nanocrystalline TiO_2 films[27] and has been inferred from fluorescence quenching experiments for an oxazine dye into SnS_2.[28] This result is however at variance the results of Kamat and co-workers, which indicate that electron injection from $Ru(dcbpy)(bpy)_2^{2+}$ into a range of different semiconductor films occurs in 2−10 ns.[15,21] It is possible that this difference indeed results from a slower rate of electron injection for this sensitizer dye, although the studies of Kamat and co-workers have been limited to a nanosecond time resolution, and further studies with an improved time resolution are necessary to establish this point.

Electron Injection versus Recombination. We find that ~50% of the electron injection occurs within our 150 fs instrument response. This high rate of electron transfer raises the possibility that this reaction proceeds adiabatically. The ultrafast electron injection kinetics are in marked contrast to the charge recombination reaction, which exhibits multiphasic kinetics on time scales up to 10^{-3} s. Thus this two-component energy storage system exhibits charge separation and recombination rates differing by up to 10^{10}.

The data presented here are limited to the observation of single sensitizer dye/semiconductor interface, and therefore a detailed discussion of the factors controlling the rates of electron injection and recombination would be premature. However, our observations, when combined with previous observations, do indicate some factors that may be of particular importance. The excited states of **1** lie above the conduction band edge for the TiO_2 (see Figure 1), and electron injection is therefore possible to a continuum of acceptor states. Under these conditions the reaction may be activationless, with the large number of possible acceptor states increasing the total electronic coupling between reactant and product states. The strong binding of this dye to the semiconductor surface and the metal-to-ligand charge-transfer character of optically excited-state transition of the dye have also been suggested to favor rapid electron injection.[5] It has been suggested that the slow rate of back-electron-transfer reaction may be associated with large free energy loss accompanying this reaction, resulting in it lying in the Marcus inverted region.[5] Other factors suggested to be important in controlling the slow rate of charge recombination include weak electronic coupling between the electron in the solid and the Ru(III) center of the dye cation and trapping of the injected electron by semiconductor surface states. Recent studies have shown that trapping of directly excited conduction band electrons by intraband surface states occurs in $\sim 10^{-13}$ s in colloidal TiO_2 particles.[29]

Relevance to Photoelectrochemical Solar Cells. Two aspects of our results are of particular relevance to further development of dye-sensitized photovoltaic cells.

(i) The ultrafast rate of electron injection is likely to be a critical factor in the excellent stability of solar cells employing this sensitizer dye. Ligand substitution reactions from the excited state of **1** have been estimated[4] to have a rate constant of the order of 10^4 s^{-1}. The electron injection rate of $\geq 10^{12}$ s^{-1} indicates that the rate of electron injection exceeds degradation pathways by $\sim 10^8$. This is consistent with recent stability studies of photoelectrochemical solar cells which indicate this dye can undergo $> 5 \times 10^7$ turnovers/molecule without loss of photovoltaic performance. Such long-term stability is essential for commercial application of this technology.

(ii) The observed rate of injection ensures that electron injection is achieved with a high quantum yield, as the rate of electron injection is 4 orders of magnitude faster than the decay rate of the dye excited state observed in solution (10^8 s^{-1}). Given the rapid injection rate observed here, it is remarkable that very few other sensitizer dyes have been identified with comparable quantum yields of electron injection. Further measurements that identify the factors that affect these competing processes will be essential for the development of new dye-sensitized thin films with improved energy conversion efficiencies.

Acknowledgment. We would like to thank Dr. Chris Barnett for excellent technical support and Stephen Merry and Richard Willis for help in the operation of the laser apparatus. J.R.D. and D.R.K. acknowledge support from the EPSRC and University of London. J.R.D. is a BBSRC Advanced Research Fellow. J.E.M. and M.G. acknowledge the support of the Swiss National Science foundation.

References and Notes

(1) Kamat, P. V. *Chem. Rev.* **1993**, *93*, 267.
(2) Tani, T. *J. Imaging Sci.* **1990**, *34*, 143.

(3) O'Regan, B.; Grätzel, M. *Nature (London)* **1991**, *353*, 737.
(4) Nazeeruddin, M. K.; Kay, A.; Rodicio, I.; Humphrey-Baker, R.; Müller, E.; Liska, P.; Vlachopoulos, N.; Grätzel, M. *J. Am. Chem. Soc.* **1993**, *115*, 6382.
(5) Hagfeldt, A.; Grätzel, M. *Chem. Rev.* **1995**, *95*, 49.
(6) Lanzafame, J. M.; Palese, S.; Wang, D.; Miller, R. J. D.; Muenter, A. A. *J. Phys. Chem.* **1994**, *98*, 11020.
(7) Levich, V. G. In *Advances in Electrochemistry and Electrochemical Engineering*; Delahay, P., Tobias, C., Eds.; Wiley: New York, 1966; Vol. 4, p 249.
(8) Willig, F.; Eichberger, E.; Sundaresan, N. S.; Parkinson, B. A. *J. Am. Chem. Soc.* **1990**, *112*, 2702.
(9) Kalyanasundaram, K. *Coord. Chem. Rev.* **1982**, *46*, 159.
(10) Carroll, P. J.; Brus, L. E. *J. Am. Chem. Soc.* **1987**, *109*, 7613.
(11) Dallinger, R. F.; Woodruff, W. H. *J. Am. Chem. Soc.* **1979**, *101*, 4391.
(12) De Armond, M. K.; Myrick, M. L. *Acc. Chem. Res.* **1989**, *22*, 364.
(13) Eichberger, R.; Willig, F. *Chem. Phys.* **1990**, *141*, 159.
(14) Willig, F.; Kietzmann, R.; Schwarzburg, K. In *Photochemical and Photoelectrocehmical Conversion and Storage of Solar Energy*; Tian, Z. W., Cao, Y., Eds.; International Academic Publishers: Beijing, China, 1993; p 129.
(15) Fessenden, R. W.; Kamat, P. V. *J. Phys. Chem.* **1995**, *99*, 12902.
(16) Hashimoto, K.; Hiramoto, M.; Kajiwara, T.; Sakata, T. *J. Phys. Chem.* **1988**, *92*, 1016.
(17) Kay, A.; Humphrey-Baker, R.; Grätzel, M. *J. Phys. Chem.* **1994**, *98*, 952.
(18) Durrant, J. R.; Tachibana, Y.; Moser, J. E.; Grätzel, M.; Klug, D. R. In *Springer Series in Chem. Phys.*, *Ultrafast Phenomena XI*; Springer-Verlag: Berlin, in press.
(19) Rech, T.; Durrant, J. R.; Joseph, D. M.; Barber, J.; Porter, G.; Klug, D. R. *Biochemistry* **1994**, *33*, 14768−14774.
(20) Noukakis, D., Moser, J. E., unpublished data.
(21) Vinodgopal, K.; Hua, X.; Dahlgren, R. L.; Lappin, A. G.; Patterson, L. K.; Kamat, P. V. *J. Phys. Chem.* **1995**, *99*, 10883.
(22) Darwent, J. R.; Kalyanasundaram *J. Chem. Soc., Faraday Trans. 2* **1981**, *77*, 373.
(23) Kosower, E. M.; Cotter, J. L. *J. Am. Chem. Soc.* **1964**, *86*, 5524.
(24) Rothenburger, G.; Fitzmaurice, D.; Grätzel, M. *J. Phys. Chem.* **1992**, *96*, 5983.
(25) O'Regan, B.; Moser, J. E.; Anderson, M.; Grätzel, M. *J. Phys. Chem.* **1990**, *94*, 8720.
(26) Stimulated emission would appear in the transient spectra as a negative signal with similar amplitude to the ground-state bleach but red-shifted from it.
(27) Rehm, J. M.; Mclendon, G. L.; Nagasawa, Y.; Yoshihara, K.; Moser, J.; Grätzel, M. *J. Phys. Chem.* **1996**, *100*, 9577.
(28) Lanzafame, J. M.; Miller, R. J. D.; Muenter, A. A.; Parkinson, B. A. *J. Phys. Chem.* **1992**, *96*, 2820.
(29) Skinner, D. E.; Colombo, D. P.; Cavaleri, J. J.; Bowman, R. M. *J. Phys. Chem.* **1995**, *99*, 7853.

JP962227F